Chinese Journal of
POLYMER SCIENCE

ARTICLE

https://doi.org/10.1007/s10118-020-2358-1
Chinese J. Polym. Sci. **2020**, *38*, 629–637

Molecular Weight Dependence of Associative Behavior in Polyimide/DMF Solutions

Hong-Xiang Chen[a,b], En-Song Zhang[a*], Mei Hong[a,b], Wei Liu[a], Xue-Min Dai[c], Quan Chen[a], Xue-Peng Qiu[c], and Xiang-Ling Ji[a,b*]

[a] *State Key Laboratory of Polymer Physics and Chemistry, Changchun Institute of Applied Chemistry, Chinese Academy of Sciences, Changchun 130022, China*
[b] *School of Applied Chemistry and Engineering, University of Science and Technology of China, Hefei 230026, China*
[c] *Laboratory of Polymer Composites and Engineering, Changchun Institute of Applied Chemistry, Chinese Academy of Sciences, Changchun 130022, China*

Electronic Supplementary Information

Abstract Eight 6FDA-TFDB polyimide (PI) samples with absolute molecular weights ranging from 1.25×10^5 g·mol^{-1} to 3.11×10^5 g·mol^{-1} are obtained by precipitation fractionation. Rheological experiments are conducted to determine the influence of molecular weight on the associating behavior of PI in *N*,*N*′-dimethylformamide (DMF) solutions in a broad volume fraction, including abnormal steady shear flow, solution heterogeneity, and scaling behavior. Abnormal flow behaviors, *i.e.*, multi-region shear thinning and weak shear thickening, are studied, and these behaviors have not been reported in literature. The heterogeneity of PI/DMF solutions is examined by dynamic rheological test. By plotting η_{sp} versus ϕ/ϕ_{η}, four concentration regions of I–IV can be distinguished for all PI samples with various molecular weights. The scaling results in different concentration regions are in good agreement with the associative polymer theory proposed by Rubinstein and Semenov. The scaling exponents do not show molecular weight dependence in concentration regions I and II. In concentration regions III and IV, the scaling exponents change little when the molecular weight is below 242 k but increase when the molecular weight increases from 242 k to 311 k. This work can help us to understand polyimide solution properties from dilute to semidilute entangled solutions, and will guide the polyimide solution preparation for different processing.

Keywords Soluble polyimide; Molecular weight; Rheology; Associative polymer; Scaling behavior

Citation: Chen, H. X.; Zhang, E. S.; Hong, M.; Liu, W.; Dai, X. M.; Chen, Q.; Qiu, X. P.; Ji, X. L. Molecular weight dependence of associative behavior in polyimide/DMF solutions. *Chinese J. Polym. Sci.* **2020**, *38*, 629–637.

INTRODUCTION

Associative polymers generally contain interactive groups that can associate with each other to form various stable structures. According to the number of associative groups along one polymer chain, three kinds of associative polymers are classified. The first kind contains one associative group, such as AB or ABA block polymers (A is the solvophilic block, and B is the associative block).[1,2] The second kind includes two associative groups, *i.e.*, telechelic polymers (BAB block polymers).[3,4] The third kind has many associative groups (*e.g.*, hydrogen bonding, electrostatic interaction, hydrophobic interaction, metal coordinate interaction) along polymer chains.[5–9] The rheological properties of associative polymers, such as gelation, shear thickening, and shear thinning, have been extensively studied.[10–13] Rubinstein and Semenov developed a theory for multisticker pair-wise associative polymers and studied the concentration dependence of viscosity at various concentration regimes.[14] Their theory fits very well in many associative polymer systems.[15–18]

Aromatic polyimides (PIs) have unique stiff backbone structure, which induces outstanding mechanical, thermal, and electrical properties.[19–22] However, the poor solubility of aromatic PIs in organic solvents and low optical transparency limit their applications. The introduction of fluoroalkyl groups can not only increase solubility but also reduce electronic interaction between color-causing groups, thus endowing PIs with high solubility and optical transparency.[23,24] Compared with the studies on synthesis process, the solution properties of PIs have not been widely studied. Many works have confirmed that PIs exhibit a random coil conformation with local rigidity in dilute solutions.[25–27] Zhang *et al.* studied the 6FDA-TFDB PI/DMF solutions over a wide concentration range using scaling theory for neutral polymers. They found that the deviation of scaling exponents of specific viscosity versus concentration is caused by the relatively weak interaction, *i.e.* dipole-dipole interaction and π-π stacking.[28] Molecular weight has important effects on the rheological properties of polymer solutions. The influence of molecular weight

* Corresponding authors, E-mail: zhangensong@fudan.edu.cn (E.S.Z.)
E-mail: xlji@ciac.ac.cn (X.L.J.)

Received August 23, 2019; Accepted September 16, 2019; Published online November 18, 2019

on the scaling relationship of viscosity and concentration for neutral polymer was studied by Gupta *et al.*[29] By observing the scaling behavior of poly(methyl methacrylate) with molecular weights from 1.247×10^4 g·mol^{-1} to 3.657×10^5 g·mol^{-1} in semidilute concentration regions, they found that the scaling exponent is independent of molecular weight. However, Zhang *et al.* drew a different conclusion when studying the scaling behavior of 6FDA-TFDB PI/DMF solution.[30] Although some deviations were found, the scaling behavior of 6FDA-TFDB PI with relatively low molecular weight in DMF solution could be explained by neutral polymer theory. They found that scaling exponents increase with molecular weight in three concentration regions, *i.e.*, dilute, semidilute unentangled, and semidilute entangled solutions. Moreover, they reported that the 6FDA-TFDB PI/DMF solution shows associative characteristics when the molecular weight is sufficiently high.[31] Therefore, we prefer to further investigate whether molecular weight (relatively high) has influence on associative behavior in PI/DMF solutions.

In the present work, 6FDA-TFDB PIs with different molecular weights are obtained by precipitation fractionation. The absolute weight-average molecular weights are measured by gel permeation chromatography (GPC) coupled with a multidetector system. Eight PI samples with different molecular weights (from 1.25×10^5 g·mol^{-1} to 3.11×10^5 g·mol^{-1}) are chosen to study the influence of molecular weight on the associative properties in DMF solution.

THEORY

Cole-Cole Plot or Han Plot

For a dynamic shear flow, the storage modulus G' and loss modulus G'' are expressed as follows: [32,33]

$$G' = \sum_{P\ \mathrm{odd}} \frac{G_0}{P^2} \frac{(\omega\lambda_P)^2}{1+(\omega\lambda_P)^2} \tag{1}$$

$$G'' = \sum_{P\ \mathrm{odd}} \frac{G_0}{P^2} \frac{\omega\lambda_P}{1+(\omega\lambda_P)^2} \tag{2}$$

in which

$$\lambda_P = \lambda_D/P^2, P = 1, 3, 5, \ldots, N \tag{3}$$

$$G_0 = ckT/M_c \tag{4}$$

where ω is the frequency, λ_P is the relaxation time spectrum, λ_D is the disengagement time, c is the constant, and M_c is the average molecular weight between entanglement points.

When a single relaxation time is considered, *i.e.*, $P = 1$, the storage modulus G' and loss modulus G'' are reduced to:

$$G' = G_0 \frac{(\omega\lambda_D)^2}{1+(\omega\lambda_D)^2} \tag{5}$$

$$G'' = G_0 \frac{\omega\lambda_D}{1+(\omega\lambda_D)^2} \tag{6}$$

At longer time scale, *i.e.* $\omega\lambda_D \ll 1$, we obtain

$$G' = (G'')^2/G_0 \tag{7}$$

By taking logarithms of the equation, we obtain

$$\log G' = 2\log G'' - \log G_0 \tag{8}$$

It shows that $\log G'$ is proportional to $\log G''$ with a slope of 2 for a single relaxation time situation. The deviation of the slope from 2 can be used to infer heterogeneity of polymer solutions.

Scaling Behavior of Associative Polymer Solution

From the theory proposed by Rubinstein and Semenov,[14] the dynamics of an unentangled associative polymer solution well above the gelation transition are described by the "sticky Rouse" model and the dynamics of an associative polymer solution above entanglement threshold can be described by the "sticky reptation" model. For the sticky Rouse model, the relaxation time τ_{Rouse} can be expressed as follows:

$$\tau_{\mathrm{Rouse}} \approx \tau_b (fP_{\mathrm{inter}})^2 \approx \tau_b f^2 l^{2+2z} \phi^{(2+2z)/(3\nu-1)} \text{ for } \phi_g \ll \phi < \phi_s \tag{9}$$

$$\tau_{\mathrm{Rouse}} \approx \tau_b (fP_{\mathrm{inter}})^2 \approx \tau_b f^2 \text{ for } \phi > \phi_s \tag{10}$$

where τ_b is the lifetime of a bond, f is the total number of stickers per chain, l is the number of monomers between neighboring stickers, ϕ_g is the gel point concentration, P_{inter} is the fraction of interchain association, and ϕ_s is the overlap concentration of the strands between stickers. The viscosity of the unentangled associative polymer solution is proportional to the modulus G_1 and the sticky Rouse time.

$$\eta \approx G_1 \tau_{\mathrm{Rouse}} \approx \left(kT\tau_b/b^3\right) N l^{2z} \phi^{1+(2+2z)/(3\nu-1)} \text{ for } \phi < \phi_s \tag{11}$$

$$\eta \approx G_1 \tau_{\mathrm{Rouse}} \approx \left(kT\tau_b/b^3\right) N l^{-2} \phi \text{ for } \phi > \phi_s \tag{12}$$

For the sticky reptation model, the reptation time is defined as follows:

$$\tau_{\mathrm{rep}} \approx \tau_b f^2 (N/N_{e0}) l^{2+2z} \phi^{(3+2z)/(3\nu-1)} \text{ for } \phi_e < \phi < \phi_s \tag{13}$$

$$\tau_{\mathrm{rep}} \approx \tau_b f^2 (N/N_{e0}) \phi^{1/(3\nu-1)} \text{ for } \phi_s < \phi < 1 \tag{14}$$

where ϕ_e is the entanglement concentration. The viscosity in this case is

$$\eta \approx G_0 \tau_{\mathrm{rep}} \approx \left(kT\tau_b/b^3\right) f^2 (N/N_{e0}) l^{2+2z} \phi^{(3+3\nu+2z)/(3\nu-1)} \text{ for } \phi_e < \phi < \phi_s \tag{15}$$

$$\eta \approx G_0 \tau_{\mathrm{rep}} \approx \left(kT\tau_b/b^3\right) f^2 \left(N/N_{e0}^2\right) \phi^{(3\nu+1)/(3\nu-1)} \text{ for } \phi_s < \phi < 1 \tag{16}$$

The detailed scaling relationships ($\eta \sim \phi^n$) in the sticky Rouse model and sticky reptation model with unrenormalized bond lifetime are summarized in Table 1.

Table 1 Relevant scaling laws ($\eta_0 \sim \phi^n$) in sticky Rouse and sticky reptation models with unrenormalized bond lifetime.

Model	Concentration range	In θ solvent	In good solvent
Sticky Rouse	$\phi_g \ll \phi < \phi_s$	3	4.2
	$\phi_s < \phi < \phi_e$	1	1
Sticky reptation	$\phi_e < \phi < \phi_s$	5.67	6.8
	$\phi_s < \phi < 1$	3.67	3.6

EXPERIMENTAL

Chemicals

2,2′-Bis(trifluoromethyl)-4,4′-diaminobiphenyl (TFDB) and 2,2-bis(3,4-di-carboxyphenyl)hexafluoropropane dianhydride (6FDA) were supplied by Beijing Multi Technology and purified by sublimation under reduced pressure. *N,N′*-dimethylacetamide (DMAc, AR) was obtained from Beijing Multi Technology and dried in the presence of P_2O_5 overnight before use. *N,N′*-dimethylformamide (DMF, HPLC) was obtained from Tedia Co.,

Ltd. Tetrabutylammonium bromide (TBAB, AR) was obtained from Sinopharm Chemical Reagent Co., Ltd.

Synthesis of Polyimide (PI)

The synthetic process is shown in Scheme 1. TFDB was dissolved in DMAc to get a homogeneous solution in a three-necked flask. Then the same molar amount of 6FDA was stirred into the flask. The mixture was reacted for 48 h at ambient temperature to get viscous poly(amic acid) solution. Nitrogen atmosphere was used to avoid the effect of ambient moisture. Chemical imidization reaction was conducted by adding triethylamine and acetic anhydride into the above poly(amic acid) solution, and the reaction was lasted for 4 h to get PI solution. The product was precipitated out and washed in excess methanol to get solid PI sample. At last, the solid PI sample was heated in a vacuum at 300 °C for 5 h to get thoroughly imidized PI sample.

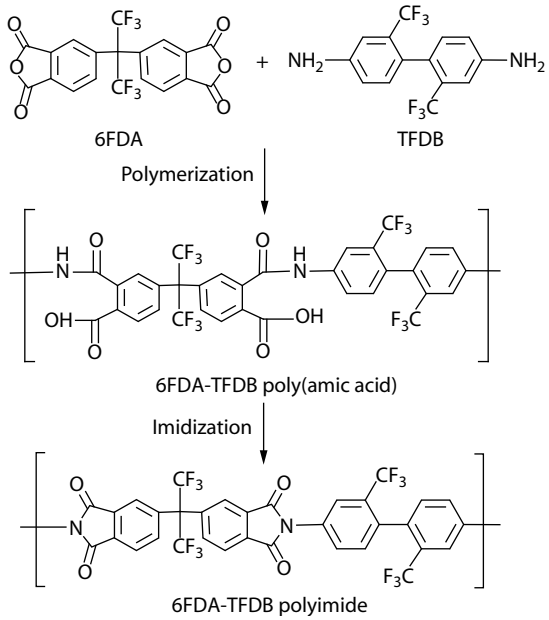

Scheme 1 Synthetic procedure of 6FDA-TFDB polyimide sample.

Fractionation of PI Sample

Approximately 20 g of PI sample was dissolved into THF to obtain approximately 1 wt% dilute solution in three-necked flask in a 25 °C water bath. As the precipitant, water was added into the solution slowly to bring it to the cloud point. To achieve the proper quantity of PI fraction, we further added an appropriate quantity of water into the solution. The turbid solution sat at least 24 h for equilibrium. The dense phase was separated by centrifuge and washed with water to obtain the solid fraction. Repeated manipulations were conducted for the dilute phase to obtain different fractions. Then, 140 g of PI sample was fractionated following the procedure above. The molecular weight and polydispersity index of the obtained fractions were measured by GPC. Similar molecular weight fractions were mixed into THF and precipitated with water. Finally, we obtained the experimental PI samples with different molecular weights.

Spectral Characterization

Fourier transform infrared (FTIR) spectra were collected on a Brucker Vertex 70 spectrometer. The solid PI sample was mixed with KBr to reduce the matrix effects. The mixture was ground to powder and pressed into a compact pellet for measurement. The FTIR spectrum of PI sample is given in Fig. S1 (in the electronic supplementary information, ESI). Adsorption bands at 1788, 1729, 718, and 1365 cm^{-1} are assigned to C=O asymmetric stretching vibration, C=O symmetric stretching vibration, C=O banding vibration, and C—N stretching vibration, respectively. Absorption bands at 3363 and 1650 cm^{-1}, which are normally characteristic bands for amide group, cannot be found. These results indicate that the polyimide was fully imidized.

^{1}H-NMR spectra were obtained on a Brucker AV400 NMR spectrometer. The ^{1}H-NMR spectrum is shown in Fig. S2 (in ESI). The resonance signals at 8.05 (d, J = 7.6 Hz, 2H), 7.94 (s, 2H), 7.87 (m, 4H), 7.68 (d, J = 8.2 Hz, 2H), and 7.44 (d, J = 8.2 Hz, 2H) confirmed the PI chemical structure. In addition, the signals of —COOH and —NH— groups cannot be found, indicating a complete imidization.

Gel Permeation Chromatography (GPC) Coupled with Multidetector

GPC was coupled with a multidetector system, including a 515 pump (Waters Tech.), a 717 autosampler (Waters Tech.), two PL-gel 10 μm Mixed B-LS columns (Agilent Tech.), a 2414 refractive index detector (Waters Tech.), and a DAWN HELEOS II multiangle laser light scattering detector (Wyatt Tech.). DMF with 3.1 mmol·L^{-1} TBAB was used as the mobile phase. The system was run at a flow rate of 1 mL·min^{-1} at 35 °C. The molecular information of samples was determined with ASTRA software. The detailed molecular weight information is listed in Table 2.

Table 2 Molecular weight information of PI samples.

Sample	Absolute $M_w \times 10^{-5}$	PDI	R_g (nm)
PI-125k	1.25	1.19	15.0
PI-145k	1.45	1.22	16.3
PI-166k	1.66	1.28	20.5
PI-195k	1.95	1.29	19.4
PI-215k	2.15	1.38	21.1
PI-242k	2.42	1.34	21.7
PI-284k	2.84	1.42	21.8
PI-311k	3.11	1.46	23.1

Rheological Measurement

PI solutions for rheological measurements were prepared by combining PI sample and DMF in a 10 mL glass vial. The mixtures were shaken for at least 72 h to allow PI to dissolve completely. Steady and oscillation experiments were performed on a TA DHR-2 stress-controlled rheometer equipped with a cone-plate geometry (2° cone angle, 40 mm diameter, 56 μm gap). Temperature was controlled using a Peltier system. Moderate amount of sample solution was transferred slowly onto a Peltier plate to avoid air bubbles. Solvent evaporation was inhibited by covering a solvent trap on the plate. The steady experiments were conducted at various temperatures from 20 °C to 45 °C.

RESULTS AND DISCUSSION

Influence of Molecular Weight on the Flow Behavior of PI/DMF Solutions

The apparent viscosities against shear rate at various volume

fractions for PI/DMF solutions with different molecular weights were examined from 20 °C to 45 °C. A representative result of PI-242k in DMF solutions at 20 °C is shown in Fig. S3 (in ESI). As shown in Fig. S3(a) (in ESI), the intrachain association is dominant, and the viscosities with shear rate suggest a Newtonian behavior in dilute PI/DMF solutions. As shown in Fig. S3(b) (in ESI), the interchain association begins to contribute to the viscosity due to the overlap of polymer chains. The disruption of interchain associations by the imposed shear deformation is replaced by new associations between various stickers. Hence, the viscosities of PI/DMF solutions are independent of shear rate. Shear thinning behavior can be seen in Fig. S3(c) (in ESI) at high shear rates. With the increase in concentration, additional interchain associations are formed. Shear thinning occurs when the rate of association disruption is greater than the rate of association formation. As shown in Figs. S3(d) and S3(e) (in ESI), the onset of shear thinning locates at the low shear rate. For entangled situations, the shear thinning becomes much more dramatic due to the disentanglement of polymer chains. Abnormal shear behavior, which is clearly shown in Fig. 1, is found in Fig. S3(d) (in ESI).

In this work, the specific viscosity of $\eta_{sp} = (\eta_0 - \eta_s)/\eta_s$ is used to establish the scaling relationship with volume fraction, where η_0 is the zero shear viscosity of polymer solutions and η_s is solvent viscosity. As shown in the concentration regions a–d in Fig. S3 (in ESI), the plateau value at low shear rates is defined as zero shear viscosity η_0. In concentration region e, zero shear viscosity η_0 is determined by the Carreau-Yasuda model:[34]

$$\frac{\eta - \eta_\infty}{\eta_0 - \eta_\infty} = \frac{1}{\left[1 + (\tau\dot{\gamma})^2\right]^{\frac{n}{2}}} \quad (17)$$

where η is the apparent viscosity, η_∞ is the infinite viscosity, τ is the relaxation time, $\dot{\gamma}$ is the shear rate, and n is the power law exponent.

Notably, special shear flow behavior can be clearly distinguished for PI samples with various molecular weights in DMF solutions. Fig. 1 shows the representative steady flow curves for PI-145k and PI-215k PI samples in DMF solutions at 20 °C. The PI-145k sample displays two shear thinning regions in the flow curves of volume fractions equal to 0.077 and 0.088 (Figs. 1a and 1b), while the flow curve of the volume fraction of 0.101 exhibits weak thickening behavior (Fig. 1c). This abnormal behavior disappears when the volume fraction is higher than 0.112. For the PI-215k sample, weak shear thickening is observed under the volume fractions of 0.077, 0.087, and 0.098 (Figs. 1e–1g), and this behavior disappears at higher volume fraction. The onset of the abnormal behavior shifts to lower shear rate as the volume fraction is increased, and the onset also appears earlier in PI-215k than in PI-145k. This result indicates that the abnormal flow behavior appears earlier at higher concentration and molecular weight. Jin *et al.* reported multi-region shear thinning in chitosan-graft-polyacrylamide aqueous solution and attributed this phenomenon to shear-induced variation of intermolecular interactions in the solution.[35] The shear thickening behavior has been observed in associative polymer solutions, suspensions, and worm-like micelles.[36] The mechanism of shear thickening for associative polymers with multiple stickers is generally ascribed to the transition of intrachain association to interchain association during shearing.[37–39] With the increase in shear rate, the intrachain associations can be destroyed due to the stretching of polymer chains, and then the interchain associations are introduced. Polymer chains will be linked to-

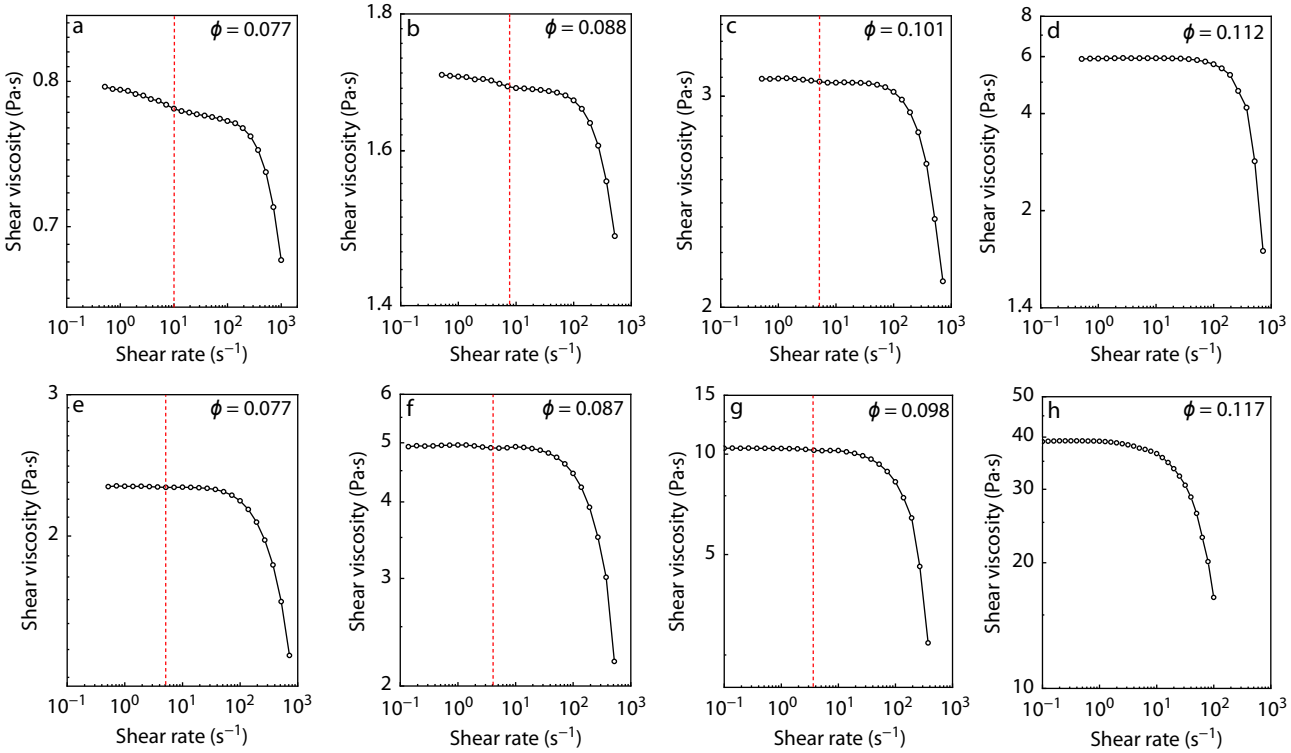

Fig. 1 The log-log plot of shear viscosity against shear rate at various volume fractions at 20 °C: (a–d) PI-145k and (e–h) PI-215k.

https://doi.org/10.1007/s10118-020-2358-1

gether by these new associations between chain units, which thereby increases the solution viscosity. In our concentrated solution, two interactions, that is, physical entanglements and dipole-dipole interactions, are included. The breakup of the physical entanglements with the increase in shear rate can decrease the apparent viscosity, while the transformation of intrachain interaction to interchain interaction can increase the apparent viscosity. The competition between these two factors results in a complex flow behavior. With increasing concentration to a critical value, shear thinning prevails due to stronger thinning process, thereby leading to the disappearance of shear thickening behavior. This is commonly found in other associative polymer solutions.[4,40] For higher molecular weight PI/DMF solutions, the destruction of intrachain associations is strengthened due to stronger orientation and disentanglement of PI chains under shear flow. Thus, shear thinning prevails, leading to the disappearance of shear thickening behavior. Finally, the mechanism of multi-region shear thinning and weak shear thickening behaviors in our system lies in the transition of intrachain association to interchain association during shear process.

Influence of Molecular Weight on the Dynamic Shear Rheological Behavior for PI/DMF Solutions

The storage modulus G' and loss modulus G'' are quantitative indications of the elastic and viscous behavior of the solutions, respectively. The variations of moduli G' and G'' with angular frequency ω for PI samples with different molecular weights at the volume fraction of 0.120 at 20 °C are shown in Fig. 2. G' is lower than G'' spanning all the range of angular frequency when the molecular weight is lower than 2.42×10^5. G' and G'' intersect at high frequency when the molecular weight is higher than 2.42×10^5, and the intersection points shift to lower frequency with increased molecular weight. Both G' and G'' drop at long time scales. However, these curves cannot be fitted by the Maxwell model, that is, $G' \sim \omega^2$ and $G'' \sim \omega^1$. For example, the slope of G' versus ω is 1.56, and the slope of G'' versus ω is 0.95 for the PI-311k solution. This deviation is commonly explained by the molecular weight distribution and the existence of physical structures.[41] Polydisperse polymers may display low frequency dependence of G' and G'' due to the broadened relaxation time caused by multiexponential decay.[42] Physical structures can also cause multiple relaxation time values in polymer solutions due to the coexistence of gel and solution. The presence of physical structures in PI/DMF solutions can be examined by log-log plotting of G' versus G'', the so-called Cole-Cole plot or Han plot. This plot is sensitive to molecular weight distribution and physical structures in solution but weakly dependent on molecular weight and concentration when entanglement effects are important.[33] This plot has been used to infer the heterogeneity of polymer solutions.[43] A slope of 2 is valid for absolutely homogeneous polymer solutions. The energy dissipation in solutions containing physical structures would increase during structural change, thereby resulting in a slope smaller than 2. Fig. 3 shows the log-log plot of G' versus G'' for PI solutions with different molecular weights at the fixed volume fraction of 0.120. The slope decreases from 1.81 to 1.59 when the molecular weight increases from 1.25×10^5 to 3.11×10^5, indicating increased physical structure or heterogeneity in these solutions. Herein, these results indicate that the deviation from Maxwell model is mainly due to the multiple relaxation time originated from the existence of the gel structure. The dipole-dipole association drags the relaxation of polymer chains, and this is more effective for high molecular weight PI chains with a larger amount of associative points than for low molecular weight PI chains with a smaller amount of associative points. This result is also confirmed by the increased activation energy with the increase in molecular weight, as shown in Fig. S4 (in ESI). Similar results have been reported in PVA solutions because of the increase of hydroxyl group interactions.[44] In addition, the Cole-Cole plot slope decreases with increasing concentration for all PI samples due to the formation of additional physical network structure.

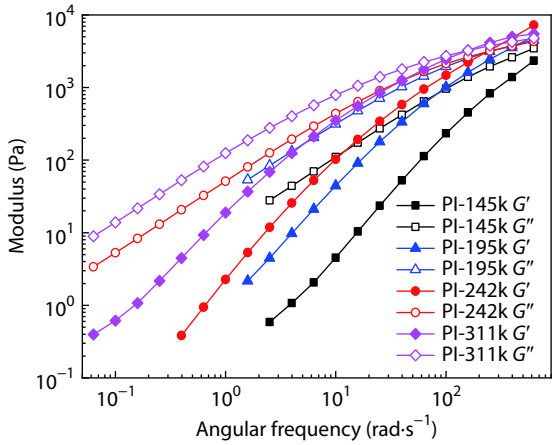

Fig. 2 Storage modulus G' and loss modulus G'' as a function of angular frequency of PI samples with different molecular weights at $\phi = 0.120$ and 20 °C.

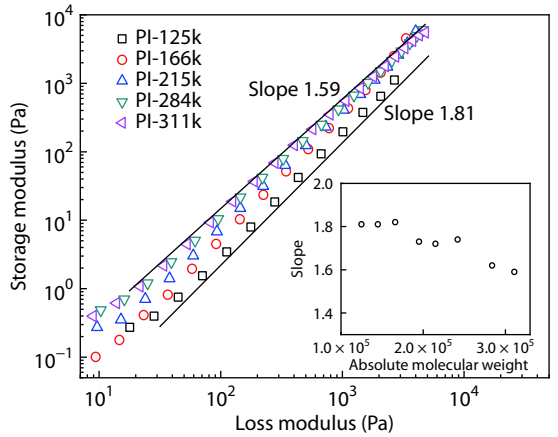

Fig. 3 The log-log plot of storage modulus G' versus loss modulus G'' of PI samples with different molecular weights at $\phi = 0.120$ and 20 °C. The inset shows the variation of slope with molecular weight.

The plots of steady shear and complex viscosities (η, η^*) versus shear rate ($\dot{\gamma}$) or frequency (ω) are shown in Fig. 4. The Cox-Merz rule[45] is followed at low shear rate or frequency $|\eta^*| = \eta$, while $\eta < |\eta^*|$ can be seen at high shear rate or frequency for PI samples with various molecular weights. This result indicates the formation of new physical structures during the shear process. The departure from Cox-Merz rule has been reported in other associative polymer solutions.[46] At a

https://doi.org/10.1007/s10118-020-2358-1

fixed volume fraction of 0.120, the critical value of $\dot{\gamma}$ or ω shifts to lower value with increasing molecular weight when Cox-Merz rule fails. Interestingly, the η data of different PI samples, when $\dot{\gamma}$ or ω is higher than the critical value, can be fitted by one linear curve with a slope of −1.06. This result could mean that the physical structures are fragmented and oriented under fast steady shear process. The orientation of these fragmented structures is somewhat similar for PI samples with different molecular weights.

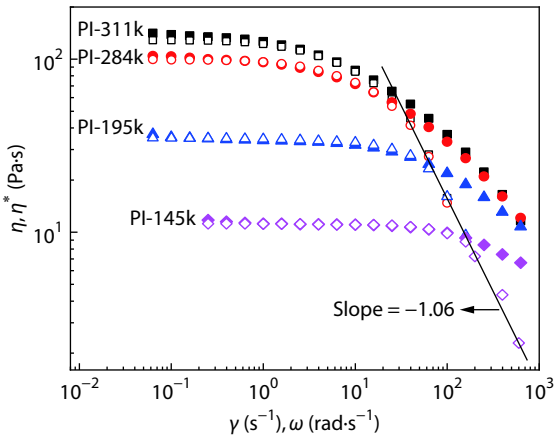

Fig. 4 Cox-Merz plot of PI in DMF with different molecular weights at ϕ = 0.120 and 20 °C. η^* and η are represented by filled and hollow symbols, respectively. Solid line represents the power-law relationship.

Influence of Molecular Weight on the Scaling Behavior of PI/DMF Solutions

On the basis of viscosity results, the relationships between η_{sp} and ϕ for different PI samples are established, as shown in Fig. 5. Obviously, the viscosity increases with increasing molecular weight. Previously, Zhang *et al.* found that the scaling behavior of 6FDA-TFDB PI/DMF solutions can be described by the sticky Rouse and sticky reptation models.[31] The intersection of dilute and semidilute concentration regions is generally defined as overlap concentration, which is widely used for neutral polymers. For neutral polymer chains, η_{sp} is proportional to the hydrodynamic volume of individual polymer chains, but this is not valid for associative polymers due to the aggregation of polymer chains. For better interpretation, we apply the concentration ϕ_η when the specific viscosity is equal to 1.0 to rescale the concentration. As shown in Fig. 5, this critical concentration ϕ_η decreases with increased molecular weight. Fig. 6(a) shows the relationship between specific viscosity η_{sp} and rescaled concentration ϕ/ϕ_η. On the basis of the scaling result, four concentration regions can be distinguished as I–IV.

(I) In the dilute region, that is, $\phi/\phi_\eta < 1$, the intrachain dipole-dipole interaction is dominant. The scaling exponent is independent of molecular weight as shown in Fig. 6(b). The associative polymer chains act independently, and increasing molecular weight will increase the intrachain interaction among polymer coils. These intrachain interactions have less impact on the solution viscosity. Hence, the scaling exponent does not change with varying molecular weight.

(II) Beyond the dilute region, η_{sp} increases gradually with ϕ/ϕ_η. In this concentration region, the experimental points for

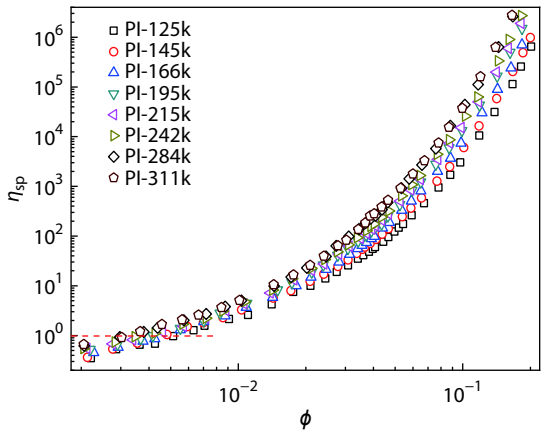

Fig. 5 Plot of specific viscosity η_{sp} against ϕ for PI samples with different molecular weights at 20 °C.

different molecular weight PI solutions almost fall in one curve. As shown in Fig. 6(c), the scaling exponents are 3.00, 2.94, 3.02, 3.01, 2.91, 3.01, 3.03, and 3.00, showing no obvious trend with the increase in molecular weight. In this region, clusters are formed by interchain dipole-dipole interactions due to the overlap of polymer chains. The solution behaves as a polydisperse cluster solution. These clusters are connected by some "bridges", resulting in the formation of a weak network structure. The solution dynamic is controlled by breaking these crucial "bridges".[47] The solution in this region shows higher concentration dependence of solution viscosity. The curves of η_{sp} versus ϕ/ϕ_η for all PI samples almost fall on one master curve, indicating that the scaling exponent has no obvious molecular weight dependence in this region.

(III) As concentration increases to region III, developed network is formed, showing a relatively high concentration dependence. Fig. 6(d) shows the relationship between the scaling exponent and molecular weight. The scaling exponents are 3.97, 3.92, 3.99, 3.97, 4.02, 4.22, 4.31, and 4.37 when the molecular weight increases from 1.25×10^5 to 3.11×10^5, which are consistent with the theoretical prediction by sticky Rouse model when $\phi_g \ll \phi < \phi_e$. The scaling exponent changes slightly at molecular weight below 2.42×10^5, but it shows an obvious increase when the molecular weight increases from 2.42×10^5 to 3.11×10^5. Cram *et al.* studied the scaling behavior of hydrophobically modified dimethylacrylamide and found that the scaling exponent of viscosity versus concentration increases with increasing hydrophobic content, that is, increasing the association strength between stickers.[17] In our system, increasing the molecular weight increases the number of stickers along polymer chains, thereby increasing the association strength between polymer chains. Thus, the scaling exponent shows an increasing trend with the further increase in molecular weight.

(IV) The crossover between regions III and IV is marked as the entanglement concentration, where polymer chains begin to entangle with each other. In concentration region IV, polymer chains are connected to the network by interchain interaction and topological entanglement, resulting in a dense network. The sticky motion of polymer chains is modified to the sticky reptation model, which allows the polymer chains to reptate along the confining "tube" formed by neigh-

https://doi.org/10.1007/s10118-020-2358-1

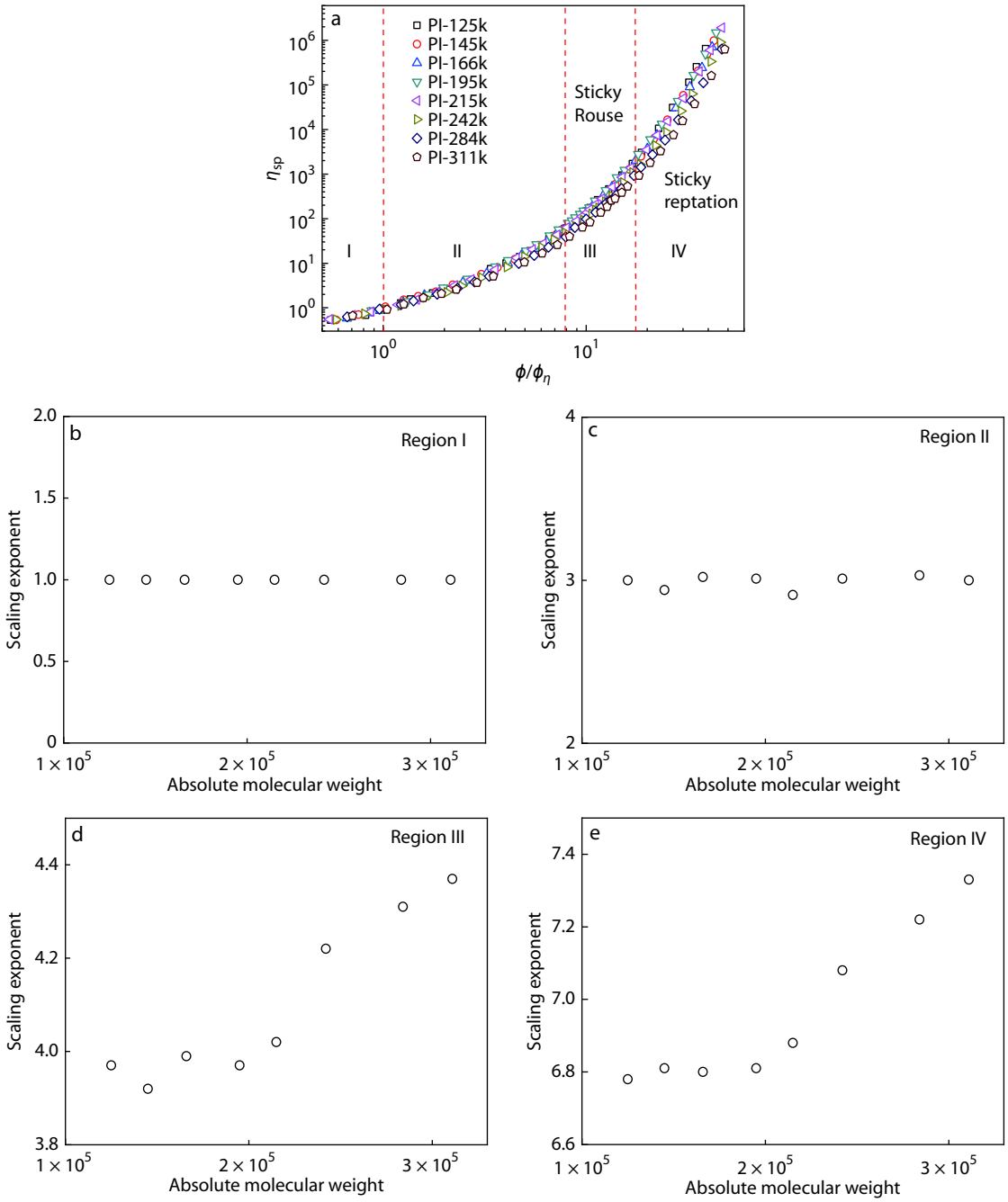

Fig. 6 (a) Scaling relationship between η_{sp} and ϕ/ϕ_η for PI samples with various molecular weights at 20 °C; (b–e) Variation of scaling exponent with molecular weight in concentration regions of I, II, III, and IV, respectively.

boring chains.[14,48] Additional intrachain interaction transforms into interchain interaction, thereby leading to the extremely strong concentration dependence of scaling exponent. The relationship between the scaling exponent and molecular weight is shown in Fig. 6(e). The scaling exponents are 6.78, 6.81, 6.80, 6.81, 6.88, 7.08, 7.22, and 7.33 when the molecular weight increases from 1.25×10^5 to 3.11×10^5, corresponding to the theoretical prediction by sticky reptation model for $\phi_e < \phi < \phi_s$. Similarly, the scaling exponent changes little when the molecular weight is below 2.42×10^5 but increases when the molecular weight increases from 2.42×10^5 to 3.11×10^5. The abnormal shear flow behavior occurs in this concentration region due to the transformation of intrachain interaction into interchain interaction under shear flow.

Both the scaling exponents in the concentration regions III and IV change little when the molecular weight is below 2.42×10^5. In fact, from the plot of η_{sp} versus ϕ/ϕ_η, the viscosity data of PI samples with molecular weight from 1.25×10^5 to 2.15×10^5 fall in one master curve spanning the whole concentrations studied. However, deviation is clearly distinguished for higher molecular weight PI samples, *i.e.*, 2.42×10^5, 2.84×10^5, and 3.11×10^5, at concentration regions III and IV.

https://doi.org/10.1007/s10118-020-2358-1

According to the theory of Rubinstein and Semenov, the theoretical regions of scaling exponent are 3–4.2 ($\phi_g \ll \phi < \phi_e$) and 5.67–6.8 ($\phi_e < \phi < \phi_s$). The scaling exponents for higher molecular weight PI samples exhibit higher value than the theoretical prediction. For our 6FDA-TFDB PI sample, each unit acts as a sticker. As mentioned above, increasing molecular weight increases the number of stickers along polymer chains, thereby increasing the association strength between polymer chains. The theory proposed by Rubinstein and Semenov assumes that one polymer chain contains many stickers with strong association strength, but the number of stickers along one chain is still lower than that in our system. With further increase in molecular weight, the association strength is largely enhanced. Thus, the scaling exponents become larger and increase with molecular weight. The molecular weight of 2.42×10^5 can be defined as a critical value, above which the association strength is largely enhanced with increasing molecular weight.

The influence of temperature on the scaling exponents is also studied. A representative result is shown in Table S1 (in ESI). The scaling exponents in different concentration regions decrease with increasing temperature. The dipole-dipole associations between polymer chains are sensitive to temperature and can be weakened at high temperatures. The conformational entropy increases with the increase in temperature, which disturbs the interaction between polymer chains. Thus, the scaling exponents decrease with the increase in temperature.

CONCLUSIONS

Eight 6FDA-TFDB PI samples with relatively high absolute molecular weights (from 1.25×10^5 to 3.11×10^5) are obtained by precipitation fractionation. Steady shear and dynamic shear experiments are conducted to explore the influence of molecular weight on the associative behavior of PI/DMF solution. Abnormal flow behaviors, *i.e.*, multi-region shear thinning and weak shear thickening, are attributed to the transformation of the intrachain dipole-dipole association into interchain association. Owing to the stronger thinning process during shear flow, these behaviors become less evident with the increase in volume fraction and molecular weight. Dynamic rheological results indicate that the heterogeneity of PI/DMF solutions increases with increasing molecular weight due to the formation of additional physical structures. The scaling relationship of η_{sp} versus ϕ/ϕ_η is studied, and four concentration regions are distinguished for all PI samples. The scaling results are explained by the theory proposed by Rubinstein and Semenov. The scaling exponents show no molecular weight dependence in concentration regions I and II. In concentration regions III and IV, the scaling exponents have little change when the molecular weight is below 2.42×10^5 but increase when the molecular weight increases from 2.42×10^5 to 3.11×10^5. The molecular weight of 2.42×10^5 can be defined as a critical value, above which the association strength is largely enhanced with increasing molecular weight. Both rheological tests and scaling results show that the associative behavior of 6FDA-TFDB PI/DMF solution is enhanced by increased molecular weight because of the increased association strength of polymer chains at higher molecular weight.

Electronic Supplementary Information

Electronic supplementary information (ESI) is available free of charge in the online version of this article at https://doi.org/10.1007/s10118-020-2358-1.

ACKNOWLEDGMENTS

This work was financially supported by the National Basic Research Program of China (No. 2014CB643604) and the National Natural Science Foundation of China (No. 51173178).

REFERENCES

1 Ogura, M.; Tokuda, H.; Imabayashi, S.; Watanabe, M. Preparation and solution behavior of a thermoresponsive diblock copolymer of poly(ethyl glycidyl ether) and poly(ethylene oxide). *Langmuir* **2007**, *23*, 9429–34.
2 Renou, F.; Benyahia, L.; Nicolai, T. Influence of adding unfunctionalized PEO on the viscoelasticity and the structure of dense polymeric micelle solutions formed by hydrophobically end-capped PEO. *Macromolecules* **2007**, *40*, 4626–4634.
3 Castelletto, V.; Hamley, I. W.; Yuan, X. F.; Kelarakis, A.; Booth, C. Structure and rheology of aqueous micellar solutions and gels formed from an associative poly(oxybutylene)-poly(oxyethylene)-poly(oxybutylene) triblock copolymer. *Soft Matter* **2005**, *1*, 138–145.
4 Suzuki, S.; Uneyama, T.; Watanabe, H. Concentration dependence of nonlinear rheological properties of hydrophobically modified ethoxylated urethane aqueous solutions. *Macromolecules* **2013**, *46*, 3497–3504.
5 Ding, K.; Wang, F.; Wu, F. Association behavior of porphyrin pendants in pH-sensitive water-soluble polymer. *Chinese J. Polym. Sci.* **2012**, *30*, 63–71.
6 Golkaram, M.; Fodor, C.; Ruymbeke, E.; Loos, K. Linear viscoelasticity of weakly hydrogen-bonded polymers near and below the sol-gel transition. *Macromolecules* **2018**, *51*, 4910–4916.
7 Candau, F.; Regalado, E. J.; Selb, J. Scaling behavior of the zero shear viscosity of hydrophobically modified poly(acrylamide)s. *Macromolecules* **1998**, *31*, 5550–5552.
8 Yang, X.; Liu, J.; Li, P.; Liu, C. Self-assembly properties of hydrophobically associative perfluorinated polyacrylamide in dilute and semi-dilute solutions. *J. Polym. Res.* **2015**, *22*, 103.
9 Xu, D.; Craig, S. L. Scaling laws in supramolecular polymer networks. *Macromolecules* **2011**, *44*, 5465–5472.
10 Li, J.; Wu, F.; Wang, E. Hydrophobically associating polyacrylamides modified by a novel self-associative cationic monomer. *Chinese J. Polym. Sci.* **2010**, *28*, 137–145.
11 Witten, T. A. Associative polymers and shear thickening. *Journal de Physique* **1988**, *49*, 1055–1063.
12 Kujawa, P.; Audibert-Hayet, A.; Selb, J.; Candau, F. Rheological properties of multisticker associative polyelectrolytes in semidilute aqueous solutions. *J. Polym. Sci., Part B: Polym. Phys.* **2010**, *42*, 1640–1655.
13 Chassenieux, C.; Nicolai, T.; Benyahia, L. Rheology of associative polymer solutions. *Curr. Opin. Colloid Interface Sci.* **2011**, *16*, 18–26.
14 Rubinstein, M.; Semenov, A. N. Dynamics of entangled solutions of associative polymers. *Macromolecules* **2001**, *34*, 1058–1068.
15 Feldman, K. E.; Kade, M. J.; Meijer, E. W.; Hawker, C. J.; Kramer, E. J. Model transient networks from strongly hydrogen-bonded polymers. *Macromolecules* **2009**, *42*, 9072–9081.
16 Regalado, E. J.; Selb, J.; Candau, F. Viscoelastic behavior of

semidilute solutions of multisticker polymer chains. *Macromolecules* **1999**, *32*, 8580–8588.
17 Cram, S. L.; Brown, H. R.; Spinks, G. M.; Hourdet, D.; Creton, C. Hydrophobically modified dimethylacrylamide synthesis and rheological behavior. *Macromolecules* **2005**, *38*, 2981–2989.
18 Kujawa, P.; Audibert-Hayet, A.; Selb, J.; Candau, F. Effect of ionic strength on the rheological properties of multisticker associative polyelectrolytes. *Macromolecules* **2006**, *39*, 384–392.
19 Ding, M. Isomeric polyimides. *Prog. Polym. Sci.* **2007**, *32*, 623–668.
20 Chisca, S.; Musteata, V. E.; Sava, I.; Bruma, M. Dielectric behavior of some aromatic polyimide films. *Eur. Polym. J.* **2011**, *47*, 1186–1197.
21 Liaw, D.; Wang, K.; Huang, Y.; Lee, K.; Lai, J.; Ha, C. Advanced polyimide materials: syntheses, physical properties and applications. *Prog. Polym. Sci.* **2012**, *37*, 907–974.
22 Dong, Z.; Feng, T.; Zheng, C.; Li, G.; Liu, F.; Qiu, X. Mechanical properties of polyimide/multi-walled carbon nanotube composite fibers. *Chinese J. Polym. Sci.* **2016**, *34*, 1386–1395.
23 Dhara, M. G.; Banerjee, S. Fluorinated high-performance polymers: Poly(arylene ether)s and aromatic polyimides containing trifluoromethyl groups. *Prog. Polym. Sci.* **2010**, *35*, 1022–1077.
24 Yang, C.; Su, Y.; Wen, S.; Hsiao, S. Highly optically transparent/low color polyimide films prepared from hydroquinone- or resorcinol-based bis(ether anhydride) and trifluoromethyl-containing bis(ether amine)s. *Polymer* **2006**, *47*, 7021–7033.
25 Liu, G.; Qiu, X.; Bo, S.; Ji, X. Chain conformation and local rigidity of soluble polyimide (II): isomerized polyimides in THF. *Chem. Res. Chin. Univ.* **2012**, *28*, 329–333.
26 Liu, G.; Qiu, X.; Siddiq, M.; Bo, S.; Ji, X. Temperature dependence of chain conformation and local rigidity of isomerized polyimides in dimethyl formamide. *Chem. Res. Chin. Univ.* **2013**, *29*, 1022–1028.
27 Savitski, E. P.; Li, F.; Lin, S. H.; Mccreight, K. W.; Wu, W.; Hsieh, E.; Rapold, R. F.; Leland, M. E.; McIntyre, D. M.; Harris, F. W.; Cheng, S. Z. D.; Wu, C. Investigation of the solution behavior of organo soluble aromatic polyimides. *Int. J. Polym. Anal. Charact.* **1997**, *4*, 153–172.
28 Zhang, E.; Dai, X.; Dong, Z.; Qiu, X.; Ji, X. Critical concentration and scaling exponents of one soluble polyimide from dilute to semidilute entangled solutions. *Polymer* **2016**, *84*, 275–285.
29 Gupta, P.; Elkins, C.; Long, T. E.; Wilkes, G. L. Electrospinning of linear homopolymers of poly(methyl methacrylate): exploring relationships between fiber formation, viscosity, molecular weight and concentration in a good solvent. *Polymer* **2005**, *46*, 4799–4810.
30 Zhang, E.; Chen, H.; Dai, X.; Liu, X.; Yang, W.; Liu, W.; Dong, Z.; Qiu, X.; Ji, X. Influence of molecular weight on scaling exponents and critical concentrations of one soluble 6FDA-TFDB polyimide in DMF solution. *J. Polym. Res.* **2017**, *24*, 47.
31 Zhang, E.; Dai, X.; Zhu, Y.; Chen, Q.; Sun, Z.; Qiu, X.; Ji, X. Associative behavior of one polyimide with high molecular weight in solution through a relatively weak interaction. *Polymer* **2018**, *141*, 166–174.
32 Doi, M.; Edwards, S. F. *The theory of polymer dynamics*. Oxford university press Inc., New York, **1986**, p. 91
33 Han, C. D.; Jhon, M. S. Correlations of the first normal stress difference with shear stress and of the storage modulus with loss modulus for homopolymers. *J. Appl. Polym. Sci.* **1986**, *32*, 3809–3840.
34 Bird, R. B.; Curtiss, C. F.; Armstrong, R. C.; Hassage., O. *Dynamics of polymeric liquids, Vol 1: Fluid mechanics*. Wiley, New York, **1987**, p. 576
35 Jin, L.; Tan, Y.; Shangguan, Y.; Lin, Y.; Xu, B.; Wu, Q.; Zheng, Q. Multi-region shear thinning for subsequent static self-thickening in chitosan-graft-polyacrylamide aqueous solution. *J. Phys. Chem. B* **2013**, *117*, 15111–21.
36 van Egmond, J. W. Shear-thickening in suspensions, associating polymers, worm-like micelles, and poor polymer solutions. *Curr. Opin. Colloid Interface Sci.* **1998**, *3*, 385–390.
37 Witten, T. A.; Cohen, M. H. Crosslinking in shear-thickening ionomers. *Macromolecules* **1985**, *18*, 1915–1918.
38 Wang, S. Q. Transient network theory for shear-thickening fluids and physically crosslinked networks. *Macromolecules* **1992**, *25*, 7003–7010.
39 Xu, D.; Liu, C. Y.; Craig, S. L. Divergent shear thinning and shear thickening behavior of supramolecular polymer networks in semidilute entangled polymer solutions. *Macromolecules* **2011**, *44*, 2343–2353.
40 Vaccaro, A.; Marrucci, G. A model for the nonlinear rheology of associating polymers. *J. Non-Newtonian Fluid Mech.* **2000**, *92*, 261–273.
41 Hackelbusch, S.; Rossow, T.; van Assenbergh, P.; Seiffert, S. Chain dynamics in supramolecular polymer networks. *Macromolecules* **2013**, *46*, 6273–6286.
42 Watanabe, H. Viscoelasticity and dynamics of entangled polymers. *Prog. Polym. Sci.* **1999**, *24*, 1253–1403.
43 Eom, Y.; Kim, B. C. Solubility parameter-based analysis of polyacrylonitrile solutions in *N*,*N*-dimethyl formamide and dimethyl sulfoxide. *Polymer* **2014**, *55*, 2570–2577.
44 Rakesh, G.; Deshpande, A. P. Rheology of crosslinking poly vinyl alcohol systems during film formation and gelation. *Rheol. Acta* **2010**, *49*, 1029–1039.
45 Cox, W. P.; Merz, E. H. Correlation of dynamic and steady flow viscosities. *J. Polym. Sci.* **1958**, *28*, 619–622.
46 Suzuki, S.; Uneyama, T.; Inoue, T.; Watanabe, H. Nonlinear rheology of telechelic associative polymer networks: shear thickening and thinning behavior of hydrophobically modifiedethoxylated urethane (HEUR) in aqueous solution. *Macromolecules* **2012**, *45*, 888–898.
47 Rubinstein, M.; Dobrynin, A. V. Associations leading to formation of reversible networks and gels. *Curr. Opin. Colloid Interface Sci.* **1999**, *4*, 83–87.
48 Leibler, L.; Rubinstein, M.; Colby, R. H. Dynamics of reversible networks. *Macromolecules* **1991**, *24*, 4701–4712.

https://doi.org/10.1007/s10118-020-2358-1